are similar to isotropic values, so the transition is certainly not z polarized. Polarized data could only be obtained for the $I\bar{4}2d$ polymorph of Ru_2But_4Cl (Figure 12).

The band appears to be of roughly equal intensity ($\epsilon \sim 2$) both $\parallel c$ and $\perp c$. Again, it is clearly not z polarized. If it were molecular x,y polarized, we would expect in the oriented gas approximation that the absorption intensity $\parallel c$ would be just twice that $\perp c$. Since the site symmetry is low, we consider our observations to be consistent with an x,y-polarized transition. Note that the temperature dependence of the band (Figures 11 and 12) is consistent with a dipole-allowed transition.

We therefore assign the band in question to a transition to one of the ^2E_g excited states. The $\nu(Ru_2)$ appears to be slightly larger than in the ground state, so the one-electron assignment $\pi^* \rightarrow \delta^*$ is reasonable. If we take the excited- and ground-state $\nu(Ru_2)$ frequencies to be 340 and 330 cm^{-1}, respectively, then the I_{10}/I_{00} intensity ratios of ~ 1 are consistent[40] with an excited-state RuRu distance that is ~ 0.06 Å shorter than that in the ground state.

The temperature dependence of this absorption band is very different from that of the $\delta \rightarrow \delta^*$ transition. While limiting low-temperature vibronic line widths are about twice as large as for $\delta \rightarrow \delta^*$, much less broadening occurs at higher temperatures. Perhaps this reflects opposite excited-state metal-metal bond distance changes; metal-halide deformations are probably involved in the $\delta \rightarrow \delta^*$ temperature dependence, and the chromophore may be insensitive to these modes if it does not increase its metal-metal bond length in the excited state.

Factor group splitting was not observed for the $\pi^* \rightarrow \delta^*$ absorption of the $I\bar{4}2d$ form of Ru_2But_4Cl (Figure 12). This is reasonable, in view of the extreme weakness of the transition, according to electric dipole coupling models.[37]

There are two absorptions that are candidates for spin-flip transitions. One of them is a sharp line at 5048 cm^{-1} (Figure 12). There is no analogous line in the near-infrared absorption spectra of the other compounds; most importantly, the spectrum of the $4/m$ polymorph of Ru_2But_4Cl does not show it. The single-crystal spectra establish that it is completely polarized $\parallel c$ ($\epsilon \sim 2$); this result suggests that the absorption is attributable to a forbidden electronic transition that has become allowed in the low site symmetry lattice of the $I\bar{4}2d$ polymorph, as pure polarization $\parallel c$ is not explicable on the basis of an oriented gas model in this lattice. It also shows high-temperature broadening (Figure 12b,c) that is much more drastic than that of absorption features attributable to vibrational overtones such as the $\sim$1750-nm cluster of lines (the third overtone of $\nu(CO_2)$, methylene deformation fundamentals at $\sim$1450 cm^{-1}). While some of the absorptions to higher energy of the 5048-cm^{-1} line might be due to vibronic side bands, they are clearly much weaker than the origin; the transition in question is vertical.

Among the various spin-flip transitions, two of them become allowed $\parallel c$ (parallel to the site C_2 axis) in the $I\bar{4}2d$ lattice; these are the transitions to $^2B_{2u}$ and $^2A_{1u}$ excited states, which are therefore possible assignments for the 5048-cm^{-1} absorption.

A second spin-flip transition is suggested from the Raman work of Clark et al.,[18] who observed Raman peaks at (low-temperature values[18b]) 1582 cm^{-1} for Ru_2But_4Cl and 1591 cm^{-1} for Ru_2Prop_4Cl. Our present vibrational analysis does not place CO stretching fundamentals near 1600 cm^{-1}. More importantly, the observed "ν(CO)" bands have half-widths of 100–200 cm^{-1} (see Figure 3 of ref 18a and Figure 7 of ref 18b). This is extraordinarily broad for a vibrational transition but reasonable for a vertical electronic transition. We therefore suggest reassignment to an electronic Raman transition.[50]

The proposed spin-flip Raman peak shows resonance enhancement,[18] indicative of a totally symmetric transition. The simplest assignment would then be the $^4B_{2u} \rightarrow {}^2B_{2u}$ spin flip. There is a complication, however. Other ruthenium carboxylates do not show strictly analogous Raman features: while $Ru_2(AcO)_4Cl$ reportedly exhibits a weak $\sim$1600-cm^{-1} line at room temperature, the feature vanishes at low temperature.[18b] This suggests that the transition is not inherently allowed (perhaps it is allowed at high temperature by a vibronic mechanism) but becomes totally symmetric in the Ru_2But_4Cl and Ru_2Prop_4Cl lattices. Clark et al.[18] appear to have studied the $I\bar{4}2d$ polymorph of the butyrate. The propionate was presumably the material that crystallizes from propionic acid, whose structure has not been established. For the $I\bar{4}2d$ butyrate, the $^4B_{2u} \rightarrow {}^2B_{2u}$ and $^2A_{1u}$ transitions become totally symmetric; thus, we place one of them at 1582 cm^{-1} and the other at 5048 cm^{-1}.

Acknowledgment. We thank R. E. Marsh and S. F. Rice for helpful discussions and D. S. Martin and R. J. H. Clark for communication of results prior to publication. This research was supported by National Science Foundation Grant CHE84-19828.

(50) (a) Clark, R. J. H.; Dines, T. J. *Adv. Infrared Raman Spectrosc.* **1982**, *9*, 282. (b) Larrabee, J. A.; Spiro, T. G. *J. Am. Chem. Soc.* **1980**, *102*, 4217.

Contribution No. 7455 from the Arthur Amos Noyes Laboratory, California Institute of Technology, Pasadena, California 91125

Electronic Spectra of Tetranuclear Linear-Chain Rhodium Isocyanide Complexes

Vincent M. Miskowski* and Harry B. Gray*

Received August 20, 1986

The electronic spectrum of the tetranuclear rhodium complex $Rh_4b_8^{6+}$ (b = 1,3-diisocyanopropane) has been studied as a function of medium and temperature. The intense absorption at $\sim$600 nm is attributed to a $\sigma \rightarrow \sigma^*$ transition within the linear Rh_4^{6+} unit. Both band-moment studies and a simple Hückel model for the metal-metal bonding indicate that the excited-state distortion is confined to an elongation of the central metal-metal bond.

A tetranuclear rhodium complex, $Rh_4b_8^{6+}$ (b = 1,3-diisocyanopropane), has been found[1] to react photochemically with protons to produce H_2. The $CoCl_4^{2-}$ salt of $Rh_4b_8^{6+}$ contains a Rh_4^{6+} linear chain with a central Rh–Rh length of 2.775 Å and outer Rh–Rh distances of 2.932 and 2.923 Å.[2] The central bond length is similar to single-bond distances found in binuclear Rh_2^{4+} (d^7–d^7) complexes of isocyanide ligands, whereas the outer bond

(1) (a) Miskowski, V. M.; Sigal, I. S.; Mann, K. R.; Gray, H. B.; Milder, S. J.; Hammond, G. S.; Ryason, P. R. *J. Am. Chem. Soc.* **1979**, *101*, 4384–4385. (b) Mann, K. R.; Gray, H. B. *Adv. Chem. Ser.* **1979**, *No. 173*, 225–235. (c) Mann, K. R.; Lewis, N. S.; Miskowski, V. M.; Erwin, D. K.; Hammond, G. S.; Gray, H. B. *J. Am. Chem. Soc.* **1977**, *99*, 5525–5526.

(2) Mann, K. R.; DiPierro, M. J.; Gill, T. P. *J. Am. Chem. Soc.* **1980**, *102*, 3965–3967.

(3) (a) Rice, S. F.; Gray, H. B. *J. Am. Chem. Soc.* **1981**, *103*, 1593–1595. (b) Rice, S. F. Ph.D. Thesis, California Institute of Technology, 1982.

0020-1669/87/1326-1108$01.50/0

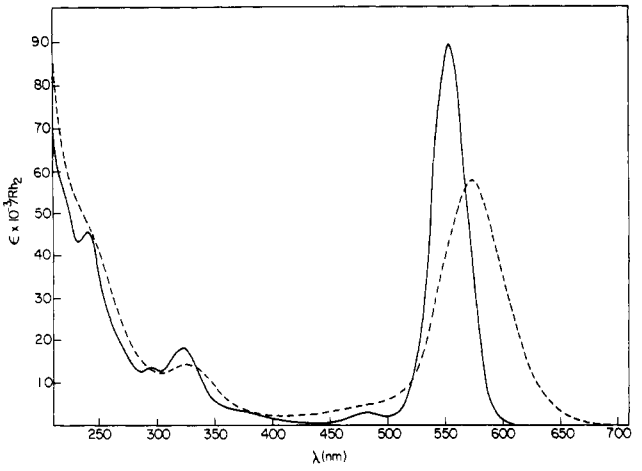

Figure 1. Absorption spectra of $Rh_4b_8^{6+}$ in 1:1 saturated LiCl(aq)–1 N H_2SO_4(aq) at 300 (--) and 70 K (—).

lengths are intermediate compared to those observed for d^7–d^7 and d^8–d^8 complexes.[4]

The $Rh_4b_8^{6+}$ complex exhibits an intense visible absorption that has been attributed to a $\sigma \rightarrow \sigma^*$ transition of the four-atom system,[1b] analogous to well-established $\sigma \rightarrow \sigma^*$ transitions of singly bonded d^7–d^7 complexes.[4] The excited state associated with the observed transition is presumably responsible for the observed photochemistry and photophysics.[1]

In this paper we report the results of extensive spectroscopic studies of $Rh_4b_8^{6+}$ in the presence of several different anions. Interpretation of these spectra has been facilitated by comparisons with data obtained previously for binuclear d^7–d^7 and d^8–d^8 analogues.[3,4]

Experimental Section

Preparation of $[Rh_2b_4](BF_4)_2$. A 10-fold excess of $[Bu_4N]BF_4$ was added to a concentrated filtered CH_3CN solution of $[Rh_2b_4](BPh_4)_2$.[1a] Cooling in a refrigerator overnight gave a precipitate, which was collected and recrystallized from hot CH_3CN. The resulting gray powder was air-dried. Anal. Calcd (found) for $[Rh_2b_4](BF_4)_2 \cdot H_2O$: C, 31.04 (30.08); H, 3.38 (3.31); N, 14.48 (14.40). If a smaller excess of BF_4^- is employed in the reaction, a mixed $(BF_4)(BPh_4)$ salt is obtained. Use of $[Rh_2b_4](BF_4)_2$ in the preparation of the tetramer is desirable, as the presence of BPh_4^- can lead to side reactions in the oxidation.

Preparation of $[Rh_4b_8](PF_6)_6$. Excess solid $[NH_4]PF_6$ was added with stirring to a concentrated 1 N H_2SO_4(aq) solution of the cation, which was obtained by dissolving $[Rh_2b_4](BF_4)_2$ in the presence of air.[1a] When the mixture was allowed to stand in the dark, a blue powder settled out. Filtration, washing with CH_3CN, and vacuum drying gave a blue solid. Anal. Calcd (found) for $[Rh_4b_8](PF_6)_6$: C, 23.61 (24.00); H, 2.38 (2.55); N, 11.02 (11.00). Salts with BF_4^- and ClO_4^- could be similarly prepared. Solutions of freshly prepared material yield electronic absorption extinction coefficients similar to those obtained by in situ oxidation of $Rh_2b_4^{2+}$.

Spectroscopic Measurements. Procedures followed those previously described.[3,4] Low-temperature spectra were corrected for solvent contraction. All reported extinction coefficients are per Rh_2 unit, in order to facilitate comparisons to binuclear systems. Many attempts were made to obtain low-temperature electronic absorption glass spectra of the aquo complex of $Rh_4b_8^{6+}$. Some results were eventually obtained in a 3:2 mixture of 1,3-dihydroxypropane and 1 N H_2SO_4(aq). Although this solvent forms a stable glass in the temperature range 50–150 K, it is metastable in the range 150–260 K, unpredictably starting to crystallize; thus, adequate data could not be obtained in the latter range. Limited data were obtained in the lower temperature range.

Electronic Absorption Spectra

Absorption spectra for the tetramer in the presence and absence of chloride are presented in Figures 1 and 2. In both cases the spectra are dominated by an extremely intense absorption system that shows drastic thermal effects. The band also shifts in the presence of chloride, which is consistent with axial ligation of the

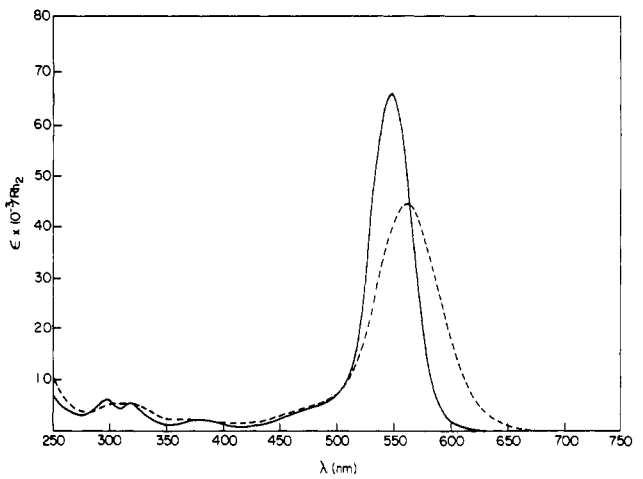

Figure 2. Absorption spectra of $Rh_4b_8^{6+}$ in 3:2 1,3-dihydroxypropane–1 N H_2SO_4(aq) at 300 (--) and 70 K (—).

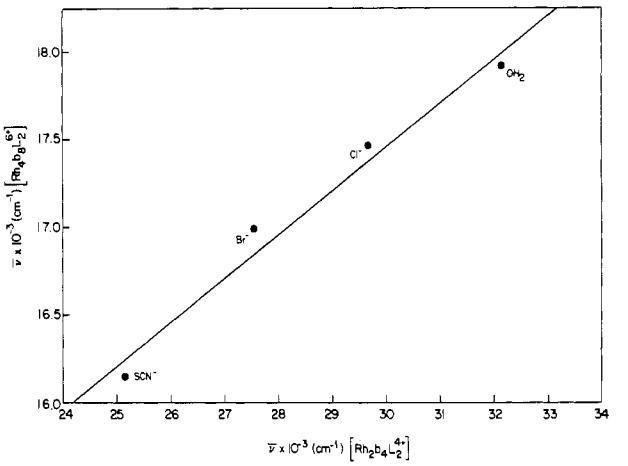

Figure 3. Correlation between $\sigma \rightarrow \sigma^*$ maxima for $Rh_4b_8L_2^{6+}$ and $Rh_2b_4L_2^{4+}$ complexes in 1 N H_2SO_4(aq), L = OH_2, Cl^-, Br^-, and SCN^-. The straight line is the linear least-squares fit, $\nu_{max}(Rh_4^{6+}) = 0.25\ \nu_{max}(Rh_2^{4+}) + 9950\ cm^{-1}$.

Table I. Data for the $\sigma \rightarrow \sigma^*$ Absorptions of $Rh_4b_8L_2^{6+}$

L	medium	λ, nm	$10^{-3}\bar{\nu}$, cm^{-1}	ϵ/Rh_2
CH_3CN	CH_3CN 10^{-2} M O_3S–C_6H_5	548	18.2	42 100
H_2O	1 N H_2SO_4(aq)	558	17.9	44 400[c]
Cl^-[a]	1 N H_2SO_4(aq)	573	17.5	57 900[d]
Br^-[a]	1 N H_2SO_4(aq)	589	17.0	66 900
SCN^-[a,b]	1 N H_2SO_4(aq)	614	16.3	75 800
I^-[a,b]	1 N H_2SO_4(aq)	622	16.1	83 300

[a] Halide or pseudohalide concentration ~0.1 M, achieved by adding sodium salt. Higher halide or pseudohalide concentrations produced negligible changes in λ_{max} and ϵ_{max}. [b] Extremely air sensitive. [c] $f = 0.43/Rh_2$; f = oscillator strength. [d] $f = 0.45/Rh_2$.

Rh_4^{6+} unit.[2] Data in the presence of high concentrations of several potential axial ligands are set out in Table I.

The trend in peak maxima is similar to that observed[4] for the $\sigma \rightarrow \sigma^*$ transition of d^7–d^7 $Rh_2b_4L_2^{n+}$ complexes,[4] as demonstrated quantitatively in Figure 3; there is a roughly linear correlation of absorption maxima. Two things are notable from the correlation. First, absorption maxima for the tetramers are about 10000 cm^{-1} lower in energy. Second, the dependence on the axial ligand is much less dramatic for the tetramers. The latter effect accords with the relatively long rhodium–chloride bonds observed in the known tetramer structure.[2] The shifts for the $Rh_2b_4L_2^{n+}$ complexes are attributable to axial ligand-to-metal charge-transfer mixing into the $\sigma \rightarrow \sigma^*$ excited state, and the strong correlation for the tetramers (Figure 3) suggests a similar mechanism, which is attenuated because of the longer bonds and the larger energy gap between $\sigma \rightarrow \sigma^*$ and the charge-transfer excited states.

(4) Miskowski, V. M.; Smith, T. P.; Loehr, T. M.; Gray, H. B. *J. Am. Chem. Soc.* **1985**, *107*, 7925–7934.

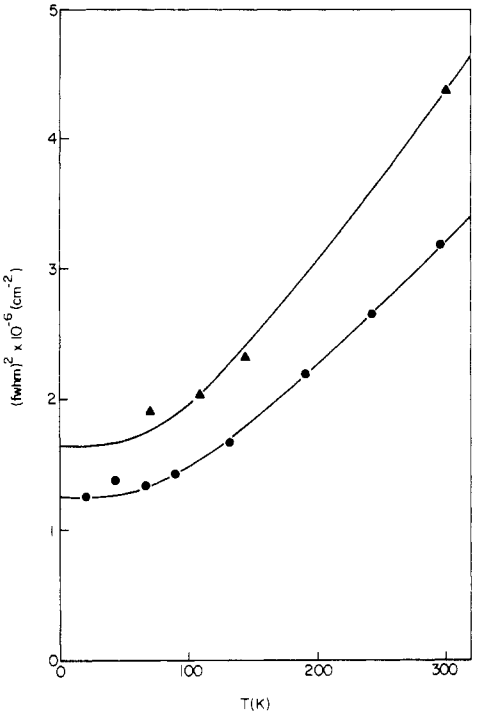

Figure 4. Second-moment fits for $Rh_4b_8^{6+}$ in LiCl glass (●) and 1,3-dihydroxypropane glass (▲).

Table II. Best-Fit Moment Parameters for $Rh_4b_8L_2^{6+}$

L	moment[a]	A	B	$\hbar\omega$, cm^{-1}
OH_2	1st	−582	18 885	250
	2nd	2.98×10^5	0	179
Cl^-	1st	−675	18 730	250
	2nd	2.29×10^5	0	175

[a] Units for A and B are cm^{-1} for the first moment and cm^{-2} for the normalized second central moment. See ref 4.

Band-Moment Analysis

Analyses of the temperature-dependent data are shown in Figures 4 and 5. The parameters obtained from fits to eq 1 (see ref 4) are given in Table II. In eq 1 $\hbar\omega$ is an effective

$$A \coth\left(\frac{\hbar\omega}{2kT}\right) + B \qquad (1)$$

ground-state vibrational frequency along whose vibrational coordinate the excited state distorts, with a magnitude of distortion related to A. Values of B have been set equal to zero for the second moment fits. Unconstrained fits gave small negative values of B, which do not have physical significance. As evidenced in Figure 4, the $B = 0$ fits are adequate for the second moments. The fits for the sparse data we have in the absence of chloride should only be taken to show that very similar parameters suffice. Since the derived effective frequencies in the presence and absence of chloride are so similar, attribution of the active mode to a metal–axial ligand vibration seems unlikely.

The effective frequencies $\hbar\omega$ that arise from the first- and second-moment fits are different, but not unreasonably so. It may be concluded from these multiparameter fits that $\hbar\omega = 210 \pm 50$ cm^{-1}; both the possibility of temperature-dependent medium effects[4] and the inherently broad[5] least-squares minima associated with eq 1 should be considered.

The ~210-cm^{-1} frequency seems reasonable for a Rh–Rh stretching mode. It is similar to (but somewhat higher than) those of ~130–160 cm^{-1} obtained[4] for similar fits to $\sigma \rightarrow \sigma^*$ data for $Rh_2b_4L_2^{n+}$ complexes, where the effective frequency was identified as ν(Rh–Rh) from Raman data. It is noteworthy that the A terms in the second-moment fits are only about 70% as large for the tetramers as for the d^7–d^7 Rh_2 complexes, suggesting smaller excited-state distortions.[4] The absence of significant B terms moreover indicates that the excitation is localized; no high-frequency modes can have significant Franck–Condon factors or else B terms would arise. It is also of interest that the first-moment A terms are considerably higher for the tetramers.

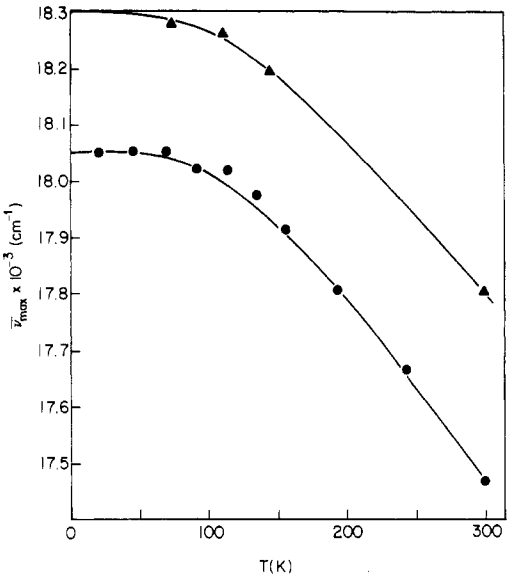

Figure 5. First-moment fits for $Rh_4b_8^{6+}$ in LiCl glass (●) and 1,3-dihydroxypropane glass (▲).

Table III. Calculated Symmetric Rh–Rh Stretching Frequencies for L–Rh_a–Rh_b–Rh_c–Rh_d–L with $d(Rh_b–Rh_c) = 2.775$ Å and $d(Rh_a–Rh_b) = d(Rh_c–Rh_d) = 2.923$ Å

L	ν_1, cm^{-1}	ν_2, cm^{-1}
none	235	95
OH_2	229	90
Cl^-	224	86

Estimation of Rh–Rh Vibrational Frequencies

Attempts to measure low-frequency vibrational spectra of $Rh_4b_8^{6+}$ compounds were uniformly unsuccessful. Both photosensitivity (Raman) and a pronounced tendency of all isolated solid compounds to smear and sinter when ground (IR) doomed these experiments. Thus the ν(Rh–Rh) values were estimated from Woodruff's correlation of metal–metal stretching frequencies and bond distances.[6] For 4d metals, Woodruff's equation is

$$d_{M_2}\,(\text{Å}) = 1.83 + 1.51 \exp(-k/2.48) \qquad (2)$$

where k is the metal–metal force constant in mdyn/Å.

The structure[2] of $Rh_4b_8^{6+}$ yields predicted force constants of 1.16 (inner Rh–Rh bond) and 0.79 mdyn/Å (outer Rh–Rh bonds). By the use of a linear four-atom force field,[7] symmetric Rh_2 vibrational frequencies were obtained (Table III); the effect of axial ligation was roughly simulated by adding the mass of the ligand to that of an outer rhodium.

The potential energy distribution shows that ν_1 and ν_2 are out-of-phase and in-phase combinations, respectively, of inner- and outer-Rh_2 bond stretching. For ν_1, the inner-bond distortion is 3.25 times as large as that for the outer bonds, so ν_1 is reasonably designated as the inner-bond stretch (similarly, ν_2 is the outer-bond stretch).

Excited-State Distortion

The predicted ν_1 of ~230 cm^{-1} is in reasonable agreement with the effective frequencies obtained from the band-moment analysis of the dominant electronic absorption. Furthermore, the moment data exclude the possibility of an active mode with a frequency near that predicted for ν_2, as considerable band-moment tem-

(5) Markham, J. J. *Rev. Mod. Phys.* **1959**, *31*, 956–989.

(6) Woodruff, W. H., to be submitted for publication.

(7) Herzberg, G. *Infrared and Raman Spectra of Polyatomic Molecules*; New York, 1945; pp 180–181.

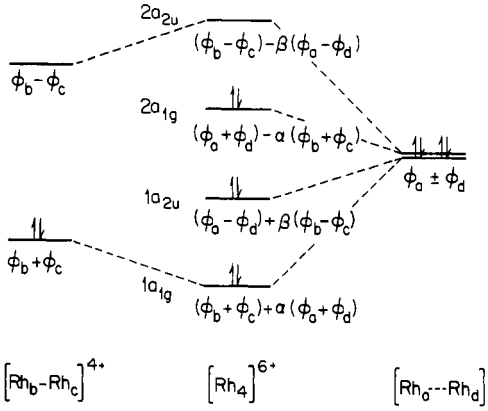

Figure 6. Molecular orbital diagram for linear $[Rh_a-Rh_b-Rh_c-Rh_d]^{6+}$. Only the d_{z^2} orbitals (ϕ_i's) of the rhodium atoms are considered. Designations are given in terms of D_{4h} symmetry.

perature dependence would otherwise result below 100 K. Accordingly, we conclude that the excited state of the electronic transition shows a large distortion only in the central Rh–Rh bond. The large first-moment A terms observed are also consistent with a distortion in the unbridged central bond; it has been suggested that anharmonicity, presumably larger for unbridged structures, is involved in determining the magnitude of the A terms.[4]

Molecular Orbital Model

A Hückel-type molecular orbital model for the tetramer that includes only the σ levels derived from metal d_{z^2} orbitals is shown in Figure 6. In the model the orbitals of a central d^7–d^7 Rh_2 unit are perturbed by two d^8 Rh "ligands". The central and outer bond orders (neglecting overlaps) are $1/(1 + \beta^2)$ and $\beta(1 + \beta^2)$, respectively. The total bond order $(2\beta + 1)/(1 + \beta^2)$ reaches a maximum at an intermediate β of $(\sqrt{5} - 1)/2 = 0.618$, so full delocalization ($\beta = 1$) is not energetically favorable.

At $\beta = 0.618$, the central and outer bond orders are 0.724 and 0.447. Thus the observed structure, with a very short central bond and outer bonds that are considerably shorter than d^8–d^8 Rh_2 distances, is consistent with the simple MO model.

Consider now the lowest energy electronic transition, $2a_{1g} \rightarrow 2a_{2u}$. Although fully allowed, this transition is not equivalent to $\sigma \rightarrow \sigma^*$ in d^7–d^7 complexes, which formally reduces the metal–metal bond order to zero. Assuming $\alpha \simeq \beta$ in the MO scheme (Figure 6), excited-state bond orders of $(1 - \beta^2)/2(1 + \beta^2)$ (central bond) and $\beta/(1 + \beta^2)$ (outer bonds) are obtained. Thus, the outer bonds are unaffected by the electronic transition in this approximation.[8] The inner bond is weakened but not broken; its bond order is 0.22 for $\beta = 0.618$. Note also that $\alpha = \beta = 0.618$ corresponds to Rh_a and Rh_b possessing 1.72 and 1.28 d_{z^2} electrons, respectively, in the ground state. In the excited state these populations are both $^3/_2$. Thus, the excited state is formed by outer → inner rhodium–rhodium charge transfer, and its electronic structure is completely delocalized.

The ground-state description accords well with the structural results.[2] The excited-state distortion is both predicted and observed to be confined to the central Rh–Rh bond and to be smaller than for the d^7–d^7 Rh_2 complexes, consistent with smaller electronic absorption bandwidths. Furthermore, the MO model is consistent with the finding that the quantum yield for the photochemical dissociation of the tetramer into Rh_2^{3+} units in aqueous sulfuric acid solution is only 0.01, which is much lower than the ~0.3 yield[9] of $Mn(CO)_5$ radicals from $\sigma \rightarrow \sigma^*$ excitation of $Mn_2(CO)_{10}$.

Other Electronic Excited States

Several relatively weak absorptions due to transitions to other electronic excited states are also evident in Figures 1 and 2.

(8) The explanation is that the outer bonds are weakened by population of $2a_{2u}$ but are simultaneously strengthened by depopulation of $2a_{1g}$.

(9) (a) Wrighton, M. S.; Ginley, D. S. *J. Am. Chem. Soc.* **1975**, *97*, 2065–2072. (b) Freedman, A.; Bersohn, R. *J. Am. Chem. Soc.* **1978**, *100*, 4116–4118.

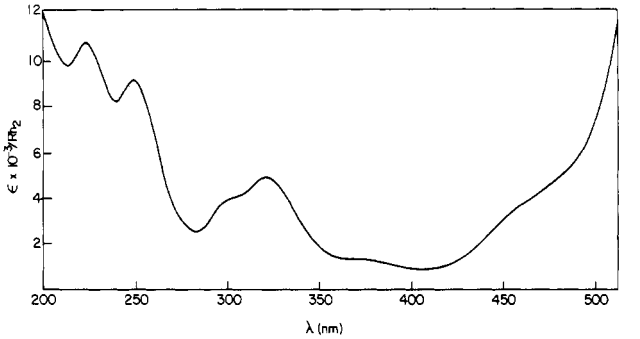

Figure 7. Absorption spectrum at room temperature of a concentrated (2.46×10^{-5} M) solution of $Rh_4b_8^{6+}$ in 1 N H_2SO_4(aq).

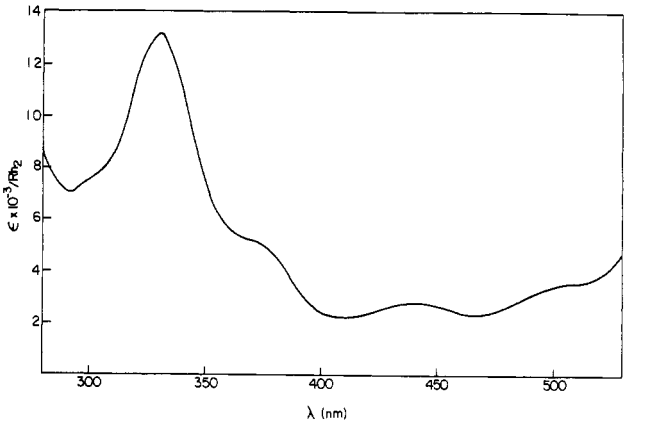

Figure 8. Absorption spectrum at room temperature of a concentrated (1.1×10^{-4} M) solution of $Rh_4b_8^{6+}$ in concentrated HBr(aq). The solution was prepared by reaction of $[Rh_2b_4](BF_4)_2 \cdot H_2O$ with degassed concentrated HBr(aq) and was triply freeze–pump–thaw degassed to remove evolved hydrogen gas. The absorption shoulder at ~370 nm could conceivably be due to trace contamination of the sample with $Rh_2b_4Br_2^{2+}$.[4]

Spectra in aqueous sulfuric acid and HBr(aq) solutions that better reveal these weak bands are shown in Figures 7 and 8.

Detailed assignments of analogous weak absorption systems of $Rh_2b_4L_2^{n+}$ complexes have been suggested. They involve transitions from $d\pi$ levels and/or excitations into $d_{x^2-y^2}$-derived orbitals. Although the spectra are difficult to analyze, it is clear that the observed absorptions occur at energies similar to those of d^7–d^7 Rh_2 complexes (features attributable to $\pi^*, \delta^* \rightarrow \sigma^*$ transitions at ~22 000–25 000 cm^{-1}, for example). Furthermore, there do not appear to be any bands similar to those of d^8–d^8 Rh_2 or mononuclear d^8 Rh complexes. (In particular, intense (ϵ/Rh_2 ~20 000–40 000) and extremely sharp features observed[3b] near 320 nm for the d^8 Rh complexes have no analogues in these spectra.) Interpretation of most of these weak bands as $d\pi$ transitions to $2a_{2u}(d\sigma^*)$ therefore seems likely. The number of electronic transitions of this type should roughly double for the tetramers (relative to the Rh_2^{4+} compounds), and this prediction is not incompatible with the data.

It has been observed previously for d^7–d^7 complexes that $d\pi \rightarrow d\sigma^*$ absorptions lose intensity at low temperature,[4] whether or not the transitions in question are formally dipole allowed, presumably because much of the transition intensity is obtained by vibronic coupling with $d\sigma \rightarrow d\sigma^*$. Most of the weak bands of the tetramers show this sort of temperature dependence.

One feature that should not lose intensity at low temperature, because it is inherently molecular z dipole allowed, is a second $d\sigma \rightarrow d\sigma^*$ transition, $1a_{1g} \rightarrow 2a_{2u}$ (Figure 6). Notice that a band at 326 nm (ϵ 14 500) in the room-temperature chloro-tetramer spectrum narrows sharply at low temperature while increasing its peak intensity (Figure 1); this is the behavior expected for a $d\sigma \rightarrow d\sigma^*$ transition. The aquo and bromo axial complexes show analogous bands at 320 (ϵ 4930) and 330 nm (ϵ 13 200). The higher energy $\sigma \rightarrow \sigma^*$ transition is expected to have lower intensity

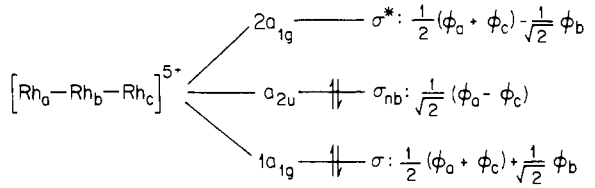

Figure 9. Molecular orbital diagram for linear $[Rh_a-Rh_b-Rh_c]^{5+}$. See the Figure 6 caption for details.

than the lower energy one, according to Mulliken.[10] If this assignment is correct, the $1a_{1g}$–$2a_{2u}$ splitting is similar to the a_{1g}–a_{2u} separation in d^7–d^7 Rh_2 compounds,[4] which is consistent with the strong central-bond description for the tetramer.

Comparisons to Related Systems

Longer-chain oligomers $[Rh_2b_4]_n^{(2n+2)+}$ have been characterized in solution.[11] The electronic structural model for these complexes closely follows that of the tetramers; a single metal–metal antibonding level is empty in the stable species, and an intense $\sigma \rightarrow \sigma^*$ transition appears at progressively lower energy as n increases.

An interesting additional case is $Rh_n^{(n+2)+}$ with n odd, in particular, the Rh_3^{5+} unit characterized by Balch and Olmstead[12] in the complex $[(C_6H_5CH_2NC)_{12}Rh_3I_2]^{3+}$. The MO diagram for Rh_3^{5+} is shown in Figure 9, where the orbitals are energetically ranked according to the number of nodes (just as for Rh_4^{6+}). The Rh–Rh bond order is $1/\sqrt{2}$ (neglecting overlap), which is consistent with the observed[12] d(Rh–Rh) = 2.796 Å. The only allowed $\sigma \rightarrow \sigma^*$ transition is $a_{2u} \rightarrow 2a_{1g}$, a nonbonding-to-antibonding transition that can also be described as outer → inner rhodium charge transfer. The observed wavelength (525 nm)[12] for the reported intense visible absorption seems reasonable for this description. (It is intermediate between the wavelengths of the bands observed for the I^- adducts of Rh_4^{6+} (Table I) and Rh_2^{4+}.[4])

A final comparison of interest is odd-electron linear-chain systems such as the platinum blues. The intense visible absorption exhibited by these materials is likely to be closely analogous to the bands under scrutiny here. A detailed experimental and theoretical study[13] of one of these materials, that containing *cis*-$[Pt(NH_3)_2(C_5H_4NO)]_4^{5+}$, is in essential agreement, although the much lower symmetry, which allows mixing among σ, π, and δ symmetry orbitals, complicates the analysis. An intense chain-polarized band at 680 nm can be assigned to a $\sigma \rightarrow \sigma^*$ transition corresponding to $2a_{1g} \rightarrow 2a_{2u}$ (Figure 6) in a hypothetical Rh_4^{5+} analogue. It is noteworthy that the geometry of the platinum tetramer, with central and outer bond lengths of 2.877 and 2.775 Å, respectively, implies $\beta > 1$ in our simple MO scheme. However, the fact that both Pt–Pt distances in the platinum tetramer are considerably longer than that of a d^7–d^7 analogue, $[Pt_2(NH_3)_4(C_5H_4NO)_2Cl_2](NO_3)_2$ with d(Pt–Pt) = 2.568 Å,[14] indicates that the Pt–Pt bonds are relatively weak. The platinum compounds appear to fall into a class of inherently shorter metal–metal bonds (for a given bond order) discussed by us elsewhere.[15] Accordingly, the small inner–outer bond length differences found in the tetranuclear platinum ion may not be relevant to the metal–metal bonding situation that prevails for the Rh_4^{6+} compounds.

Acknowledgment. We thank Woody Woodruff for several helpful discussions, especially ones in connection with ref 6. This research was supported by National Science Foundation Grant CHE84-19828.

(10) Mulliken, R. S. *J. Chem. Phys.* **1939**, *7*, 121–135.
(11) (a) Sigal, I. S.; Mann, K. R.; Gray, H. B. *J. Am. Chem. Soc.* **1980**, *102*, 7252–7256, (b) Sigal, I. S.; Gray, H. B. *J. Am. Chem. Soc.* **1981**, *103*, 2220–2225.
(12) Balch, A. L.; Olmstead, M. M. *J. Am. Chem. Soc.* **1979**, *101*, 3128–3129.
(13) Ginsberg, A. P.; O'Halloran, T. V.; Fanwick, P. E.; Hollis, L. S.; Lippard, S. J. *J. Am. Chem. Soc.* **1984**, *106*, 5430–5439.
(14) Hollis, L. S.; Roberts, M. M.; Lippard, S. J. *Inorg. Chem.* **1983**, *22*, 3637–3644.
(15) Miskowski, V. M.; Schaefer, W. P.; Sadeghi, B.; Santarsiero, B. D.; Gray, H. B. *Inorg. Chem.* **1984**, *23*, 1154–1162.

Contribution No. 7489 from the Arthur Amos Noyes Laboratory, California Institute of Technology, Pasadena, California 91125, and Mechanical and Chemical Systems Division, Jet Propulsion Laboratory, California Institute of Technology, Pasadena, California 91109

Electronic Spectroscopy of d^8–d^8 Diplatinum Complexes. $^1A_{2u}(d\sigma^* \rightarrow p\sigma)$, $^3E_u(d_{xz},d_{yz} \rightarrow p\sigma)$, and $^{3,1}B_{2u}(d\sigma^* \rightarrow d_{x^2-y^2})$ Excited States of $Pt_2(P_2O_5H_2)_4^{4-}$

Albert E. Stiegman,[†] Steven F. Rice,[†] Harry B. Gray,*[†] and Vincent M. Miskowski*[‡]

Received September 24, 1986

Polarized electronic spectral measurements have been made on single crystals of $(n\text{-}Bu_4N)_4[Pt_2(P_2O_5H_2)_4]$, and the solution photophysical properties of the $^1A_{2u}(d\sigma^* \rightarrow p\sigma)$ excited state have been studied. The $^{1,3}A_{2u}(d\sigma^* \rightarrow p\sigma)$ excited states have closely comparable excited-state distortions (largely a metal–metal contraction). Absorptions near 35 000 cm^{-1} attributable to transitions to singlet and triplet $d\sigma^* \rightarrow d_{x^2-y^2}$ excited states have been identified by their polarizations and large half-widths. Bands assigned to triplet components of $d_{xz},d_{yz} \rightarrow p\sigma$ excitations are at slightly higher energy; the extreme narrowness (500 cm^{-1} for the transition to $E_u(^3E_u)$) of these absorption systems indicates that the excited states in question are not distorted.

Numerous spectroscopic and photophysical studies on $Pt_2(P_2O_5H_2)_4^{4-}$ (D_{4h} Pt_2P_8 coordination unit) have appeared recently.[1-3] Of primary interest has been the long-lived (9.8 μs for room-temperature aqueous solution[1b]) and highly emissive $^3A_{2u}(d\sigma^* \rightarrow p\sigma)$ excited state with some attention[1c,d] also given to the weakly luminescent $^1A_{2u}(d\sigma^* \rightarrow p\sigma)$ state. Remarkable photochemistry has been observed[3,4] for the $^3A_{2u}$ excited state of this d^8–d^8 Pt_2 species.

With the aim of elucidating the $^1A_{2u}$ and other upper excited states, we have prepared and characterized the n-Bu_4N^+ salt of $Pt_2(P_2O_5H_2)_4^{4-}$. Extremely thin crystals of this compound are readily obtained, and polarized electronic absorption measurements

[†] Arthur Amos Noyes Laboratory.
[‡] Jet Propulsion Laboratory.

(1) (a) Fordyce, W. A.; Brummer, J. G.; Crosby, G. A. *J. Am. Chem. Soc.* **1981**, *103*, 7061–7064. (b) Che, C.-M.; Butler, L. G.; Gray, H. B. *J. Am. Chem. Soc.* **1981**, *103*, 7796–7797. (c) Rice, S. F.; Gray, H. B. *J. Am. Chem. Soc.* **1983**, *105*, 4571–4575. (d) Bär, L.; Gliemann, G. *Chem. Phys. Lett.* **1984**, *108*, 14–17. (e) Isci, H.; Mason, W. R. *Inorg. Chem.* **1985**, *24*, 1761–1765.
(2) Shimizu, Y.; Tanaka, Y.; Azumi, T. *J. Phys. Chem.* **1984**, *88*, 2423–2425.
(3) (a) Heuer, W. B.; Totten, M. D.; Rodman, G. S.; Hebert, E. J.; Tracy, H. J.; Nagle, J. K. *J. Am. Chem. Soc.* **1984**, *106*, 1163–1164. (b) Bryan, S. A.; Dickson, M. K.; Roundhill, D. M. *J. Am. Chem. Soc.* **1984**, *106*, 1882–1883. (c) Peterson, J. R.; Kalyanasundaram, K. *J. Phys. Chem.* **1985**, *89*, 2486–2492.

0020-1669/87/1326-1112$01.50/0